DOI: 10.1002/chem.201602980

Nanocrystal Synthesis

5-(2-Mercaptoethyl)-1*H*-tetrazole: Facile Synthesis and Application for the Preparation of Water Soluble Nanocrystals and Their Gels

Sergei V. Voitekhovich,*[a] André Wolf,[b] Chris Guhrenz,[b] Alexander S. Lyakhov,[a] Ludmila S. Ivashkevich,[a] Marion Adam,[c] Nikolai Gaponik,[b] Stefan Kaskel,[c] and Alexander Eychmüller[b]

Abstract: A facile method for the preparation of the novel capping ligand 5-(2-mercaptoethyl)-1*H*-tetrazole for the stabilization of water-soluble nanocrystals was developed. This effective synthetic procedure is based on the cycloaddition of sodium azide to 3,3′-dithiobis(propionitrile) followed by the reductive cleavage of a S–S bond with triphenylphosphine. The structure of the synthesized compound was confirmed by single-crystal X-ray analysis. A target tetrazole was successfully applied for the direct aqueous synthesis of CdTe and Au nanocrystals. CdTe nanocrystals capped with 5-(2-mercaptoethyl)-1*H*-tetrazole were found to reveal high photoluminescence efficiencies (up to 77 %). Nanocrystals capped with this tetrazole ligand are able to build 3D structures in a metal-ion-assisted gelation process in aqueous solution. Critical point drying of the as-formed hydrogels allowed the preparation of the corresponding aerogels, while preserving the mesoporous structure.

Introduction

Tetrazole derivatives have received much attention in the recent years in the field of nanostructured materials.[1] This interest is due to the unique combination of miscellaneous properties of these seemingly exotic polynitrogen compounds. First, it is the donor character of the tetrazole ring that determines the ability of tetrazoles to form stable metallocomplexes as well as to stabilize colloidal nanocrystals (NCs).[2–4] Second, it is a specific thermally induced fragmentation of the tetrazole ring leading to the formation of a high proportion of volatile products like nitrogen, nitrenes, azides, and others.[5,6] In consequence of these features, the easily available 1-alkyltetrazole-5-thiols (**1**) (Figure 1) were studied as suitable capping ligands for semiconductor (CdS,[7] $CuInSe_2$, $CuIn_{1-x}Ga_xSe_2$[8]) and noble metal (Au,[9] Ag, Pd, Pt[10]) NCs. Corresponding stable NCs were prepared by solution-phase organic syntheses,[7,9,10] including ligand exchange strategies,[8] or by a solid-phase single-precursor approach based on the thermal decomposition of tetrazole-5-thiolates.[7] As previously shown, using tetrazoles **1** as ligands opens up a straightforward opportunity to obtain highly conductive, closely assembled, and organic-free nanocrystalline solids that have great potential in photovoltaic and catalytic applications.[8] A thermolytic approach was also applied for the preparation of nanoporous metal foams with remarkably high surface areas by using metal tetrazolates as metal precursors as well as foaming agents.[11] Moreover, tetrazole derivatives were found to be useful as nitrogen precursors for the preparation of nitrogen-enriched carbon nanotubes by heating the tetrazoles with multiwalled carbon nanotubes.[12]

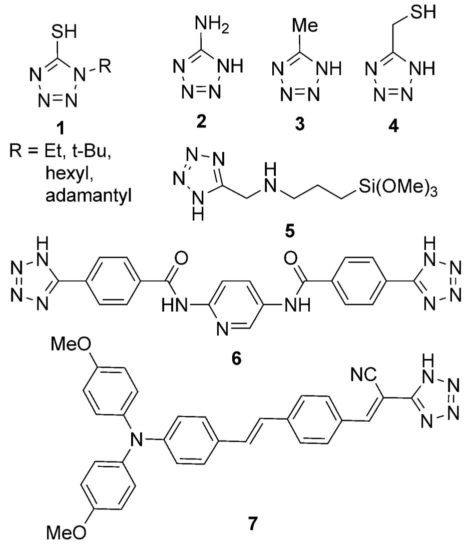

Figure 1. Tetrazole derivatives used for the preparation and functionalization of NCs (colloidal nanocrystals).

---

[a] Dr. S. V. Voitekhovich, Dr. A. S. Lyakhov, Dr. L. S. Ivashkevich
Research Institute for Physical Chemical Problems
Belarusian State University
Leningradskaya 14, Minsk 220006 (Belarus)
E-mail: azole@tut.by

[b] A. Wolf, C. Guhrenz, Prof. Dr. N. Gaponik, Prof. Dr. A. Eychmüller
Physical Chemistry, TU Dresden
Bergstr. 66b, 01062 Dresden (Germany)

[c] M. Adam, Prof. Dr. S. Kaskel
Inorganic Chemistry, TU Dresden
Bergstr. 66, 01062 Dresden (Germany)

Supporting information and ORCID(s) for the author(s) of this article can be found under http://dx.doi.org/10.1002/chem.201602980.

Due to the hydrophilic nature of the heteroring, tetrazoles are of great interest in the preparation of water-soluble nanocrystals. 5-Monosubstituted tetrazoles, being nonclassical analogs of carboxylic acids,[13] are most attractive for such purposes. Therefore, 5-aminotetrazole (**2**) and 5-methyltetrazole (**3**) were applied for an aqueous synthesis of Ag NCs.[14] Although the as-prepared NCs show a quite broad size distribution, they are of interest due to their controllable agglomeration accompanied with drastic changes in the optical properties. 5-(1-Mercaptomethyl)-1*H*-tetrazole (**4**) was found to be a good substitute for thioglycolic acid widely used as a capping agent in the aqueous synthesis of colloidal semiconductor NCs; the use of **4** allows to prepare water soluble CdTe[15] and ZnSe[16] NCs. The CdTe NCs obtained are characterized by a strong luminescence with a quantum yield of up to 60%.

It should be noted that NCs capped with tetrazole **4** possess the unique ability to reversibly form hydrogels upon addition of metal salts.[15–17] After forming the gels, the CdTe NCs preserve their absorption and photoluminescence properties, although their emission is markedly quenched. The metal-assisted gelation of tetrazole-capped NCs can also be employed to integrate different types of NCs to tune the emission of the resulting gel. Such an approach has been proposed for the gelation of NCs covered by silica shells. For these purposes, silica shells were functionalized with tetrazole **5**, which has the ability to bind to the silica surface by a silane group.[18]

Very recently, a new sensitive method for the colorimetric detection of Al^{3+}, based on the complexation of tetrazole **4** capped gold NCs with the detected cations in aqueous media, was reported.[19] Interaction of Ag^{+} ions with tetrazole **6** in water was found to produce a hydrogel with spherical silver NCs attached to the gel fibers.[20] These NCs effectively catalyze the reduction of nitro groups by borohydride, acting as an electron relay system. Moreover, the applicability of the tetrazole functional groups as an efficient anchoring group for organic photosensitizers in hybrid materials for energy applications was demonstrated in the photosensitization of TiO_2 nanoparticles using the tetrazole **7**.[21]

Therefore, in spite of the relatively short history of studies of tetrazoles as ligands and precursors in nanochemistry, quite interesting and promising results have been obtained. The prepared nanomaterials have great potential for applications in catalysis, hydrogen storage, optical sensing devices, field effect transistors, switches, solar cells, and exchange spring magnets. Progress in the synthetic chemistry of tetrazole derivatives stimulates further design and study of tetrazole-capped nanomaterials. Herein, in continuation of our previous studies concerned with the aqueous synthesis of NCs,[15–17] we present 5-(2-mercaptoethyl)-1*H*-tetrazole (**8**) as a novel capping ligand for the preparation of water soluble NCs. This ligand is an alternative to its homologue **4** as well as thioglycolic and 3-mercaptopropionic acids that are frequently used in the preparation and functionalization of NCs.[22]

Results and Discussion

Preparation and characterization of the ligand 8

In a previous work we reported the synthesis of the ligand **4**,[15] which is a homologue of the tetrazole **8** differing only by one methylene group (Scheme 1). For the synthesis of **4**, we started from the available chloroacetonitrile **9**. A cycloaddition of an in situ generated aluminium azide to the above nitrile in THF leads to the formation of 5-chloromethyl-1*H*-tetrazole (**10**). The subsequent treatment of **10** with thiourea generates the thiouronium salt **11**, which can be transformed to the tetrazole **4** under boiling with aqueous sodium hydroxide. The main disadvantage of the above approach is the necessity to use a substantial excess (3 equiv) of sodium azide, which generates the toxic and explosive hydrazoic acid during the synthetic work-up procedure. Moreover, by applying this methodology to **8**, a substitution of chlorine by a thiol group can be accompanied with the dehydrohalogenation of the intermediate 5-(2-chloroethyl)-1*H*-tetrazole to form 5-vinyl-1*H*-tetrazole as a byproduct. Taking these circumstances into account, herein, we develop another synthetic strategy for the preparation of **8**, which is described below.

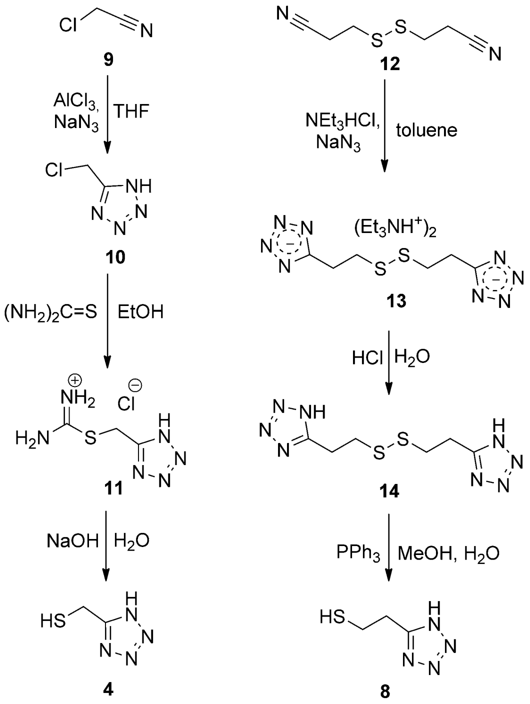

Scheme 1. Synthetic routes for the formation of the tetrazole ligands **4** and **8**.

Commercial 3,3′-dithiobis(propionitrile) (**12**) was used as a starting compound (Scheme 1). Transformation of the nitrile group into tetrazol-5-yl was successfully carried out using an adapted Koguro procedure,[23] which is based on the reaction of nitrile with sodium azide and triethylammonium chloride under reflux in toluene. The advantage of this process is its experimental simplicity, including the product isolation. The formed triethylammonium salt **13** can be extracted straight from the reaction mixture into water. The following acidification leads to the tetrazole **14,** which is insoluble in water and can be easily separated by filtration in 93% yield. Several reducing agents were tested for the cleavage of the S–S bonds in **14**. Zn/HCl and $NaBH_4$ were found to be ineffective and, as a consequence, the obtained tetrazole **8** was significantly contaminated with **14** together with some other byproducts. Triphenylphosphine in MeOH/H_2O (8:1) was found to be a convenient and effective agent for the reduction of **14**. The cleavage of the S–S bonds was achieved by stirring of the reaction mixture under reflux for 3 h with an 89% yield of **8**.

The structures of **8** and **14** were confirmed by ^{1}H and ^{13}C NMR spectroscopy. It should be noted that the NMR spectra were recorded from freshly prepared samples, since the tetrazole **8** undergoes a slow oxidation to give **14** when stored in [D$_6$]DMSO as well as in other solvents. At the same time, the crystalline **8** is air stable. No impurity of **14** was found by NMR and powder X-ray diffraction (PXRD) experiments after the sample storage under air for a week. All peaks of the experimental PXRD pattern of **8** matched well with those of the simulated one, which indicates the phase purity of the crystalline **8** (Figures S1 and S2 in the Supporting Information).

Single-crystal X-ray analysis was carried out for **8**. The crystal data and structure refinement details for this compound, investigated at 100 and 296 K, are presented in Table 1. As follows from the X-ray data, the molecular and crystal structures of **8** are practically the same at the two temperatures. Figure 2 shows the molecular structure of the tetrazole **8** at 100 K, which crystallizes in the monoclinic space group $P2_1/c$ with four molecules in the unit cell. The tetrazole ring geometry of the compound is typical for 5-monosubstituted tetrazoles. The intermolecular hydrogen bonds N1–H1···N4^{b} (symmetry transformation: b) $x, \frac{1}{2}-y, z-\frac{1}{2}$) between neighboring molecules are responsible for the formation of polymeric chains running along the *c* axis (Figure 3). There are also weak hydrogen bonds S1–H1S···N3^{a} (symmetry transformation: a) $1-x, -y, 1-z$) connecting the above chains into polymeric layers parallel to the *bc* plane.

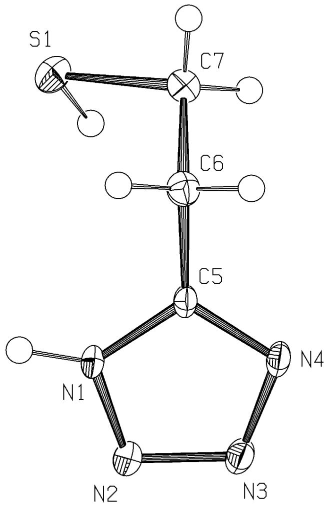

Figure 2. ORTEP-3 drawing of **8** (100 K) with displacement ellipsoids drawn at the 50% probability level. The hydrogen atoms are shown as spheres of arbitrari radii. Selected bond lengths (Å): N1–C5 1.3388(14), N1–N2 1.3486(13), N2–N3 1.2969(13), N3–N4 1.3611(14), N4–C5 1.3248(14), S1–C7 1.8152(13), C5–C6 1.4869(16), C6–C7 1.5281(17).

Table 1. Crystal data and structure refinement details for **8**.[a]

Empirical formula	$C_3H_6N_4S$	
formula weight	130.18	
wavelength [Å]	0.71073	
crystal size [mm]	0.50×0.26×0.07	
crystal system	monoclinic	
space group	$P2_1/c$	
T [K]	100	296
a [Å]	8.30940(10)	8.3776(2)
b [Å]	7.01100(10)	7.16620(10)
c [Å]	9.8814(2)	9.8995(2)
β [°]	90.9822(10)	90.8258(11)
V [Å^3]	575.578(16)	594.26(2)
Z	4	4
D_{calcd} [g cm^{-3}]	1.502	1.455
μ [mm^{-1}]	0.451	0.437
reflections collected	6263	6684
independent reflections	1691	1756
restraints	0	0
parameters	97	79
R_1/wR_2 [for $I>2\sigma(I)$]	0.0309/0.0919	0.0405/0.1244
R_1/wR_2 [all data]	0.0332/0.0944	0.0511/0.1356
goodness of fit	1.023	1.033

[a] Supplementary crystallographic data for **8** can be found in ref. [35].

In spite of the high nitrogen content (≈43%), tetrazole **8** shows a moderate thermal stability. According to the thermogravimetric (TG) and differential scanning calorimetry (DSC) curves (Figure S3), the reported compound melts at 102.5 °C. A noticeable weight loss starts at about 150 °C. Further heating

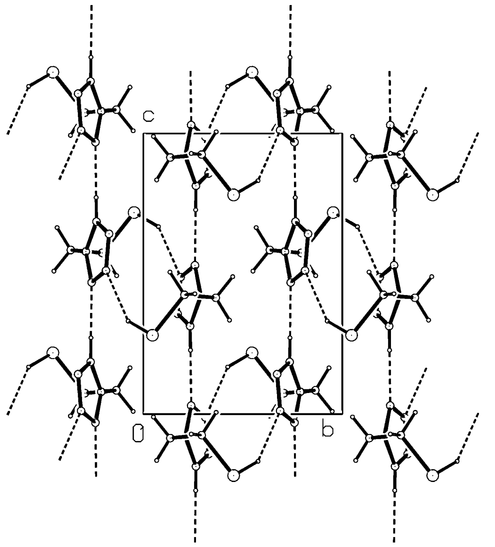

Figure 3. Crystal packing of **8** (100 K) viewed along the *a* axis. Dashed lines indicate hydrogen bonds.

up to 500 °C is accompanied by roughly 92% weight loss and one exothermic peak at 267 °C.

Nanocrystals capped with 5-(2-mercaptoethyl)-1*H*-tetrazole

Over the last decade, the great potential of tetrazoles as stabilizing agents in the synthesis of colloidal semiconductor quantum dots has been demonstrated.[1,22] Quantum dots stabilized in this way possess superior properties, such as strong photoluminescence, long term stability, compatibility with biological media, and the ability to assemble. Till now, mainly thiols having short alkylene chains with terminal hydrophilic groups (NH_2, OH, COOH) have been employed in the aqueous synthesis of metal chalcogenide NCs. The typical synthetic protocols for the preparation of these NCs includes an initial reaction of the chalcogen precursor with a metal–thiol complex that was generated in situ from a metal salt and a free ligand. Nucleation and growth of the NCs is achieved by heating (reflux) under open-air conditions and the size is controlled by the heating duration.

Following the above approach, we applied the tetrazole **8** as a capping ligand for the preparation of CdTe quantum dots. The growth of CdTe NCs was monitored by UV/Vis absorption and photoluminescence (PL) emission spectroscopy (Figure 4 and Figures S4 and S5 in the Supporting Information). Already after 5 min under reflux, the CdTe NCs, which show a green band-edge emission with a PL maximum at roughly 500 nm, are formed. Further treatment under reflux allows the NCs to grow and achieve a red emission. The PL bands of the CdTe NCs are sufficiently narrow (FWHM (full width at half maximum) values lie in the range of 32–37 nm, Figure S6), which indicates a narrow size distribution of the NCs. According to transmission electron microscopy (TEM), the average NCs size is 2.6 nm after 51 h under reflux of the reaction mixture (Figure 5).

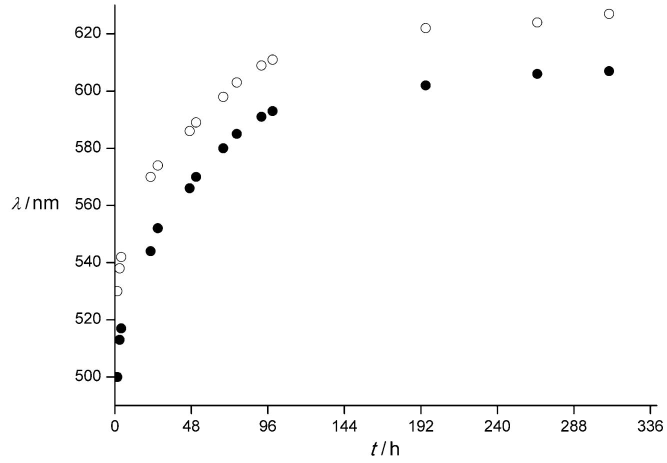

Figure 4. Temporal evolution of the UV/Vis absorption (●) and the PL emission (○) peak positions of CdTe NCs capped with tetrazole **8** under continuous reflux of the reaction mixture during the synthesis.

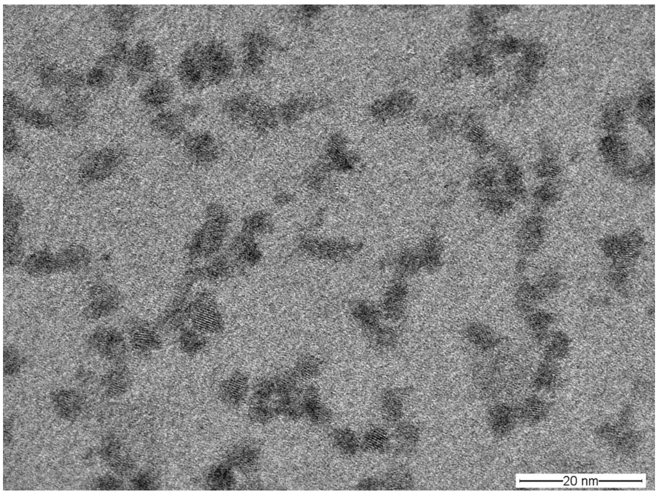

Figure 5. TEM image of CdTe NCs capped with ligand **8** after 51 h under reflux of the reaction mixture.

Comparing the behavior of the tetrazoles **4**[15] and **8** in the aqueous synthesis of CdTe NCs, we can conclude that the introduction of an additional methylene group between the thiol and the tetrazole groups results in a slight change in the growth rate, but significantly enhanced the PL quantum efficiency (QE). Whereas a QE of 60% was achieved using ligand **4**, the novel ligand **8** produces CdTe NCs with a QE of up to 77%. The increase in the QE can be explained by a change in the coordination properties of the ligand **8** compared to **4**, caused by the introduction of an additional methylene group. This methylene group can decrease the stability of the chelate cadmium–thiolate complexes, formed in the first stage of the synthesis (Figure 6). It is well known that complexes containing five-membered chelate rings are significantly more stable than complexes with six-membered chelate rings.[24] Cadmium–thiolate complexes that are present in the ligand shell, significantly affect the optical properties of the quantum dots, as reported for the colloidal synthesis of NCs in the presence of thioglycolic acid.[25] Moreover, the six-membered chelate complex can more easily undergo hydrolysis under reflux, increasing the amount of sulfur in the NCs, which can be seen in the selected area electron diffraction pattern (Figure S7). This may be the reason for such a strong QE enhancement, as was discussed in previous studies.[26,27]

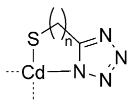

Figure 6. Probable chelate fragment of cadmium–thiolate complexes formed during the synthesis of CdTe NCs capped with tetrazoles **4** (*n* = 1) and **8** (*n* = 2).

It was found in the present work that the tetrazole **8** is suitable for the stabilization of metal NCs as well. In particular, the reduction of tetrachloroauric acid with sodium borohydride in the presence of tetrazole **8** yields spherical Au NCs with an average size of 2.7 ± 0.6 nm. Moreover, Au NCs with a size of 2.4 ± 0.7 nm were prepared using **14** instead of **8** under analogous conditions. In this case, ligand **8** is generated in situ by splitting of the S–S bond of **14** upon the addition of sodium borohydride as reducing agent. TEM images of the obtained Au NCs are presented in Figures S8 and S9 in the Supporting Information. Figure S10 shows UV/Vis spectra of the freshly prepared Au NCs. The absorption spectrum of the Au NCs prepared in the presence of ligand **8** displays a broad peak at about 515 nm, which results from the surface plasmon band of gold. However, the absorption spectrum of the Au NCs synthesized by using **14** exhibits no plasmon band. This spectral difference is due to the strong size dependence of the 5d–6sp interband transition and also additional charge–transfer effects between the NCs and the capping ligands.

It should be noted that colloidal solutions of the NCs capped with tetrazole **8** show an excellent stability. Therefore, the optical properties of the CdTe NCs have not changed upon storage of the samples under air for months. The as-prepared Au NCs showed no color changes or precipitation under analogous conditions.

Metal-assisted assembly of nanocrystals

Recently,[15–17] we found that the addition of an aqueous solution containing transition metal cations (Cd^{2+}, Zn^{2+}) to colloidal Au, CdTe, and ZnSe NCs capped with tetrazole **4** leads to the formation of hydrogels, which are formed within relatively short times (from a few seconds up to weeks, depending on the amount of the salt added). Furthermore, this facile approach for the formation of NC assemblies was applied for the preparation of hybrid metal/semiconductor and mixed semiconductor-I/semiconductor-II three-dimensional structures with controllable and tunable compositions. These assemblies can be preserved by critical point drying. The as-received highly porous aerogels are interesting materials due to their energy- and charge-transfer properties.[15–18]

Here, we examined the ability of tetrazole-stabilized NCs capped with **8** to gelate under the action of metal ions. We found that the addition of an aqueous solution of zinc acetate (10^{-2} M) to colloidal CdTe NCs capped with **8** led to the formation of hydrogels (Figure S11). Similar observations were made for Au NCs as well. A plausible mechanism for the gel formation is the cross-linking of separate NCs by the complexation of tetrazolate units with metal cations as shown in Figure 7. This mechanism is very similar to that of the formation of tetrazolate coordination polymer gels[28,29] under interaction of 5-monosubstituted tetrazoles with an excess of metal salts. Since the tetrazolate anion can act as mono-, di-, tri-, or tetradentate ligand,[2,4] any endocyclic nitrogen atom of **8** can bind with the metal cation under gelation. The coordination by the $N^2(N^3)$ atom is favored due to steric reasons.

The as-prepared hydrogels were further dried by critical point drying, yielding the corresponding aerogels. Nitrogen physisorption measurements showed the porous structure of the obtained aerogels. For the Au aerogel, a total pore volume of 0.85 $cm^3 g^{-1}$ and a specific surface area of 195 $m^2 g^{-1}$ have been determined. These values are significantly higher in comparison with those for the aerogels prepared previously using **4** as a ligand (0.51 $cm^3 g^{-1}$ and 50 $m^2 g^{-1}$, correspondingly).[17] The difference can be explained by the different size of the initial NCs as well as by the structural distinction between the ligands **4** and **8**. The isotherm acquired for the investigated aerogel is similar to type IV according to the IUPAC classification with a hysteresis of type H4, which indicates a mesoporous structure of the material with additional micropores (Figure S12).

For a pure CdTe aerogel, a specific surface area of 87 $m^2 g^{-1}$ was determined. This result proves the crucial role of the tetrazole unit in the metal-ion-assisted gelation process and the suitability of the novel ligand **8** for the preparation of 3D assemblies of colloidal NCs, which are of great interest as objects for studies in photophysics and catalysis.[17,30]

Conclusions

We have developed a facile route for the preparation of 5-(2-mercaptoethyl)-1*H*-tetrazole, which is a promising ligand for the stabilization of metal and semiconductor nanocrystals in

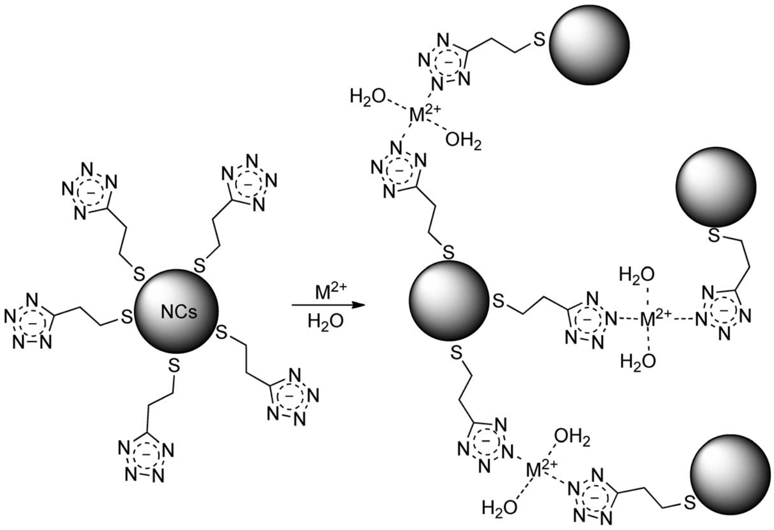

Figure 7. Gelation mechanism of the NCs capped with tetrazole **8** in the presence of metal cations.

water. Being more accessible in comparison with its homologue 5-mercaptomethyl-1*H*-tetrazole, the novel ligand shows a similar behavior in the aqueous synthesis of nanocrystals and considerably improves the photoluminescence quantum efficiency of the prepared CdTe quantum dots. The presence of a tetrazolyl moiety capable of metal binding, determines the ability of the nanocrystals capped with 5-(2-mercaptoethyl)-1*H*-tetrazole for a metal-ion-assisted gelation, which can be used for the preparation of assemblies of colloidal nanocrystals including hydrogels and aerogels with mesoporous structures.

Experimental Section

General information. All reagents were used as received from commercial sources. Milli-Q ultrapure water (Millipore Co., USA) was employed as the solvent for the preparation of the NCs. ^{1}H and ^{13}C NMR spectra were recorded on a Bruker Avance-500 spectrometer. The TG and DSC curves were obtained with a NETZSCH STA429 thermoanalyzer under a dynamic nitrogen atmosphere (heating rate 10 °C min^{-1}, aluminum oxide, mass 5–6 mg, RT–500 °C).

Synthesis of 1,2-bis(2-(1*H*-tetrazol-5-yl)ethyl)disulfane (14). Triethylammonium chloride (12.4 g, 90 mmol) and sodium azide (5.85 g, 90 mmol) were added to a solution of 3,3′-dithiobis(propionitrile) (**12**, 5.3 g, 31 mmol) in toluene (100 mL) and the mixture was stirred under reflux for 24 h. After cooling the reaction mixture to room temperature, distilled water (100 mL) was added, the aqueous layer was separated, and the toluene layer was washed with water (3×50 mL). The joint aqueous layers were acidified to pH 2 using conc. hydrochloric acid. The precipitate was filtered off, washed with water, and dried in a vacuum oven to give a cream-colored powder. Yield: 93 % (7.5 g, 29 mmol). ^{1}H NMR (500 MHz, [D$_6$]DMSO): $\delta = 3.13$ (t, J(H,H) = 7.0 MHz, 2H, CH$_2$), 3.27 ppm (t, J(H,H) = 7.0 MHz, 2H, CH$_2$); ^{13}C NMR (125 MHz, [D$_6$]DMSO): $\delta = 22.86$ (CH$_2$), 34.42 (CH$_2$), 154.44 ppm (C$_{ring}$); elemental analysis calcd (%) for $C_6H_{10}N_8S_2$ (258.33): C 27.90, H 3.90, N 43.38, S 24.83; found: C 27.75, H 4.05, N 43.10, S 24.98.

Synthesis of 5-(2-mercaptoethyl)-1*H*-tetrazole (8). A solution of **14** (2.0 g, 7.7 mmol) and triphenylphosphine (2.6 g, 10 mmol) in methanol (40 mL) and water (5 mL) was refluxed for 3 h. After cooling to room temperature, the reaction mixture was diluted with water (200 mL), and aqueous NaOH (50 %) was added until reaching pH 8–9. A precipitate containing triphenylphospine oxide and unreacted triphenylphosphine was removed by filtration. The filtrate was acidified to pH 2 using conc. hydrochloric acid. Afterwards, the solvents were evaporated and the residue was extracted with hot chloroform (200 mL). The addition of toluene (20 mL) to the extracts followed by slow evaporation of the solution gave colorless crystals of **8**. Yield: 89 % (1.78 g, 13.7 mmol); m.p. 101–102 °C. ^{1}H NMR (500 MHz, [D$_6$]DMSO): $\delta = 2.56$ (t, $J = 8.1$ MHz, 1H, HS), 2.88 (q, J(H,H) = 7.2 MHz, 2H, CH$_2$), 3.17 ppm (t, J(H,H) = 7.1 MHz, 2H, CH$_2$); ^{13}C NMR (125 MHz, [D$_6$]DMSO): $\delta = 21.49$ (CH$_2$), 27.45 (CH$_2$), 155.5 ppm (C$_{ring}$); elemental analysis calcd (%) for $C_3H_6N_4S$ (130.17): C 27.68, H 4.65, N 43.04, S 24.63; found: C 27.40, H 4.45, N 42.88, S 24.70.

Preparation of CdTe NCs capped with 5-(2-mercaptoethyl)-1*H*-tetrazole. Tetrazole **8** (0.344 g, 0.72 mmol) and cadmium(II) perchlorate hexahydrate (1.000 g, 2.38 mmol) were dissolved in water (250 mL) under stirring, followed by adjusting the pH to 11.5 by dropwise addition of aqueous NaOH (1 M). The resulting solution was placed into a flask, fitted with a septum and valves, and flushed with argon for 45 min. Under stirring, H_2Te gas (generated by the reaction of 0.300 g, 0.69 mmol Al_2Te_3 pellets with an excess amount of 1 N H_2SO_4) was passed through the solution together with a slow argon flow for 45 min. Further refluxing under argon led to the nucleation and growth of the CdTe NCs.

Preparation of Au NCs capped with 5-(2-mercaptoethyl)-1*H*-tetrazole. The ligand, namely tetrazole **14** (7.8 mg, 30 µmol) or **8** (7.8 mg, 60 µmol), was dissolved in water (20 mL), followed by the addition of aqueous NaOH (1 M, 100 µL) and 50 mM $HAuCl_4$ (200 µL). A dropwise addition of a freshly prepared, aqueous $NaBH_4$ solution (50 mM, 400 µL), accompanied with a color change from yellow to brown, indicates the formation of Au NCs. To remove byproducts and agglomerates, the reaction mixture was concentrated under reduced pressure, and the obtained residue was washed with 2-propanol and redissolved in water.

X-ray structure determination. Single crystals of **8** suitable for X-ray analysis were obtained by crystallization from chloroform/toluene (10:1). X-ray data were collected at 100 and 296 K on a SMART APEX II diffractometer using graphite-monochromated Mo$_{K\alpha}$ radiation ($\lambda = 0.71073$ Å). The reflection data were corrected on absorption. The structures were solved by direct methods with the program SIR2011[31] and refined on F^2 by the full-matrix least-squares technique with SHELXL 2014.[32] All nonhydrogen atoms were refined in anisotropic approximation. The tetrazole ring H atom and the thiole H atom were found from the difference Fourier map and refined independently in isotropic approximation. The methylene H atoms were placed in calculated positions and refined using a "riding" model with $U_{iso}(H) = 1.2\,U_{eq}(C)$. Molecular graphics was performed with the programs ORTEP-3 for Windows[33] and PLATON.[34] Supplementary crystallographic data for **8** can be found in ref. [35]. Powder X-ray diffraction (PXRD) was used to control the purity of the polycrystalline samples **8** and **14**. The powder patterns were recorded with an EMPYREAN diffractometer using Cu$_{K\alpha}$ radiation (Ni filter) at 296 K.

Nitrogen adsorption characterization. Nitrogen physisorption measurements were performed at 77 K on a Quadrasorb (Quantachrome Instrument). Prior to the measurement, the sample was evacuated at 423 K for 24 h. High purity gas was used (nitrogen: 99.999 %). Specific surface areas were calculated using the Brunauer–Emmett–Teller (BET) equation in a relative pressure range of 0.05–0.20 p/p_0. The total pore volume was determined at 0.99 p/p_0.

Quantum efficiency determination. The quantum efficiency of the CdTe NCs capped with 5-(2-mercaptoethyl)-1*H*-tetrazole were measured using a Horiba Fluorolog 3 equipped with a Quanta-Φ and a PPD-850 detector (HORIBA Scientific). The sample was excited at 550 nm. The excitation spectra were measured using a neutral-density filter 2.0 in a range of 540–560 nm with an increment of 0.1 nm and an integration time of 1 s. The emission spectra were measured in a range of 560–660 nm with an increment of 1 nm as well as an integration time of 1 s. For blank measurements, the same cuvette and solvent, but without NCs, were used. The measurements were carried out two times to reduce experimental errors. The results of the experiments are summarized in Table S1 in the Supporting Information.

Transmission electron microscopy and selected area electron diffraction. Samples were prepared by dropping diluted colloidal nanocrystals in water/acetone 1:1) on a holey graphene oxide TEM grid with subsequent evaporation of the solvent. TEM imaging was carried out on a LIBRA 120 microscope (high voltage of 120 kV) and a Tecnai T20 (FEI) electron microscope with an acceleration voltage of 200 kV, equipped with a LaB$_6$ cathode. Images and selected area electron diffraction (SAED) patterns were recorded with the software iTEM. SAED patterns were evaluated with the software ImageJ (https://imagej.nih.gov/ij/index.html) and the Radial Profile Plot plugin (http://rsb.info.nih.gov/ij/plugins/radial-profile.html) written by Paul Baggethun. First, the region of interest in the SAED pattern was distinguished with a circular selection and then the image data were radially integrated using the plugin. The gained output consisted of a two-dimensional data array that was normalized to averaged intensity versus *d* spacing.

Acknowledgements

This work was supported by the DFG project EY16/10-2 and partly by the M-ERA.NET project ICENAP (GA1289/3-1). S.V.V. acknowledges the support of research fellowships from the Alexander von Humboldt Foundation (Alumni Program). We thank Matthias Werheid (TU Dresden) for acquiring the SAED patterns.

Keywords: gels · nanocrystals · nitrogen heterocycles · porous materials · quantum dots

[1] S. V. Voitekhovich, V. Lesnyak, N. Gaponik, A. Eychmüller, *Small* **2015**, *11*, 5728 – 5739.
[2] G. Aromí, L. A. Barrios, O. Roubeau, P. Gamez, *Coord. Chem. Rev.* **2011**, *255*, 485 – 546.
[3] A. Ilie, K. Karaghiosoff, *Phosphorus Sulfur Silicon* **2011**, *186*, 389 – 403.
[4] P. N. Gaponik, S. V. Voitekhovich, O. A. Ivashkevich, *Russ. Chem. Rev.* **2006**, *75*, 507 – 539.
[5] A. I. Lesnikovich, S. V. Levchik, A. I. Balabanovich, O. A. Ivashkevich, P. N. Gaponik, *Thermochim. Acta* **1992**, *200*, 427 – 441.
[6] G. Fischer, G. Holl, T. M. Klapotke, J. J. Weigand, *Thermochim. Acta* **2005**, *437*, 168 – 178.
[7] S. V. Voitekhovich, D. V. Talapin, C. Klinke, A. Kornowski, H. Weller, *Chem. Mater.* **2008**, *20*, 4545 – 4547.
[8] J. Lauth, J. Marbach, A. Meyer, S. Dogan, C. Klinke, A. Kornowski, H. Weller, *Adv. Funct. Mater.* **2014**, *24*, 1081 – 1088.
[9] M. N. Nichick, S. V. Voitekhovich, A. Shavel, A. I. Lesnikovich, O. A. Ivashkevich, *Polyhedron* **2009**, *28*, 3138 – 3142.
[10] M. N. Nichick, S. V. Voitekhovich, V. Lesnyak, V. E. Matulis, R. A. Zheldakova, A. I. Lesnikovich, O. A. Ivashkevich, *J. Phys. Chem. C* **2011**, *115*, 16928 – 16933.
[11] B. Tappan, S. Steiner, E. Luther, *Angew. Chem. Int. Ed.* **2010**, *49*, 4544 – 4565; *Angew. Chem.* **2010**, *122*, 4648 – 4669.
[12] A. Morozan, P. Jégou, M. Pinault, S. Campidelli, B. Jousselme, S. Palacin, *ChemSusChem* **2012**, *5*, 647 – 651.
[13] R. J. Herr, *Bioorg. Med. Chem.* **2002**, *10*, 3379 – 3393.
[14] C. Ziegler, M. Klose, S. V. Voitekhovich, N. Gaponik, A. Eychmüller, *Z. Phys. Chem.* **2011**, *225*, 363 – 371.
[15] V. Lesnyak, S. V. Voitekhovich, P. N. Gaponik, N. Gaponik, A. Eychmüller, *ACS Nano* **2010**, *4*, 4090 – 4096.
[16] A. Wolf, V. Lesnyak, N. Gaponik, A. Eychmüller, *J. Phys. Chem. Lett.* **2012**, *3*, 2188 – 2193.
[17] V. Lesnyak, A. Wolf, A. Dubavik, L. Borchardt, S. V. Voitekhovich, N. Gaponik, S. Kaskel, A. Eychmüller, *J. Am. Chem. Soc.* **2011**, *133*, 13413 – 13420.
[18] C. Rengers, S. V. Voitekhovich, S. Kittler, A. Wolf, M. Adam, N. Gaponik, S. Kaskel, A. Eychmüller, *Nanoscale* **2015**, *7*, 12713 – 12721.
[19] D. Hue, H. Wang, Y. Zhang, *Talanta* **2014**, *119*, 306 – 311.
[20] J. H. Lee, S. Kang, J. Y. Lee, J. H. Jung, *Soft Matter* **2012**, *8*, 6557 – 2563.
[21] J. Massin, L. Ducasse, T. Toupance, C. Olivier, *J. Phys. Chem. C* **2014**, *118*, 10677 – 10685.
[22] V. Lesnyak, N. Gaponik, A. Eychmüller, *Chem. Soc. Rev.* **2013**, *42*, 2905 – 2929.
[23] K. Koguro, T. Oga, S. Mitsui, R. Orita, *Synthesis* **1998**, 910 – 914.
[24] R. D. Hancock, *J. Chem. Educ.* **1992**, *69*, 615 – 621.
[25] S. Leubner, S. Hatami, N. Esendemir, T. Lorenz, J.-O. Joswig, V. Lesnyak, S. Recknagel, N. Gaponik, U. Resch-Genger, A. Eychmüller, *Dalton Trans.* **2013**, *42*, 12733 – 12740.
[26] A. L. Rogach, T. Franzl, T. A. Klar, J. Feldmann, N. Gaponik, V. Lesnyak, A. Shavel, A. Eychmüller, Y. P. Rakovich, J. F. Donegan, *J. Phys. Chem. C* **2007**, *111*, 14628 – 14637.
[27] B. Haobo, G. Yanjun, L. Zhen, G. Mingyuan, *Chem. Mater.* **2004**, *16*, 3853 – 3859.
[28] H. Lee, S. H. Jung, W. S. Han, J. H. Moon, S. Kang, J. Y. Lee, J. H. Jung, S. Shinkai, *Chem. Eur. J.* **2011**, *17*, 2823 – 2827.
[29] H. Lee, S. Kang, J. Y. Lee, J. H. Jung, *Soft Matter* **2012**, *8*, 2950 – 2955.
[30] W. Liu, A.-K. Herrmann, N. C. Bigall, P. Rodriguez, D. Wen, M. Oezaslan, T. J. Schmidt, N. Gaponik, A. Eychmüller, *Acc. Chem. Res.* **2015**, *48*, 154 – 162.
[31] M. C. Burla, R. Caliandro, M. Camalli, B. Carrozzini, G. L. Cascarano, C. Giacovazzo, M. Mallamo, A. Mazzone, G. Polidori, R. Spagna, *J. Appl. Crystallogr.* **2012**, *45*, 357 – 361.
[32] G. M. Sheldrick, *Acta Crystallogr. Sect. C* **2015**, *71*, 3 – 8.
[33] L. J. Farrugia, *J. Appl. Crystallogr.* **1997**, *30*, 565 – 566.
[34] A. L. Spek, *Acta Crystallogr. Sect. D* **2009**, *65*, 148 – 155.
[35] CCDC 1414881 (**8**, 296 K), and 1414882 (**8**, 100 K) contain the supplementary crystallographic data for this paper. These data are provided free of charge by The Cambridge Crystallographic Data Centre.

Received: June 22, 2016

FULL PAPER

Nanocrystal Synthesis

S. V. Voitekhovich, A. Wolf, C. Guhrenz, A. S. Lyakhov, L. S. Ivashkevich, M. Adam, N. Gaponik, S. Kaskel, A. Eychmüller*

■■ – ■■

5-(2-Mercaptoethyl)-1*H*-tetrazole: Facile Synthesis and Application for the Preparation of Water Soluble Nanocrystals and Their Gels

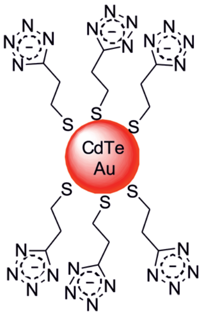

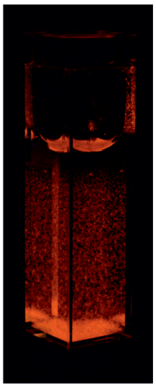

A simple ligand with huge impact! A novel tetrazole-based capping ligand was designed and applied for the direct aqueous synthesis of semiconductor and metal nanocrystals. Nanocrystals capped with tetrazole ligands are capable for a metal-ion-assisted assembly to give corresponding hydrogels and aerogels with mesoporous structures.